ELSEVIER

Journal of Molecular Catalysis A: Chemical 139 (1999) 315–323

JOURNAL OF MOLECULAR CATALYSIS A: CHEMICAL

Roles of cerium oxide and the reducibility and recoverability of the surface oxygen species in the $CeO_2/MgAl_2O_4$ catalysts

Jin-an Wang [a,*], Li-fang Chen [a], Cheng-lie Li [b]

[a] *Institute of Physics, The National University of Mexico (UNAM), P.O. Box 20-364, 01000 Mexico, D.F., Mexico*
[b] *Petroleum Processing Research Center, East China University of Science and Technology, 200237 Shanghai, China*

Received 23 January 1998; accepted 5 June 1998

Abstract

The properties of surface oxygen species in the $MgAl_2O_4$ and $CeO_2/MgAl_2O_4$ catalysts were investigated by the temperature-programmed reduction (TPR) technique. Three different oxygen species existing on the surface of $CeO_2/MgAl_2O_4$ catalysts—surface adsorbed oxygen, surface lattice oxygen which was affected by the interaction between the supported cerium and carrier, and the oxygen species corresponding to the multilayer crystalline of CeO_2, were determined. The supported cerium oxide had different functions: it not only increased the amount of surface adsorbed oxygen, but also reduced the reduction temperature of surface lattice oxygen and improved the recoverability of the surface oxygen species. These roles of cerium oxide in the $CeO_2/MgAl_2O_4$ catalyst significantly affected on the SO_2 adsorption properties, in the both cases of gaseous oxygen absence and presence in the reaction stream, enhancing the De–SO_2 activity.

Keywords: Sulfur-transfer catalyst; Cerium oxide; Magnesium–alumina spinel; Surface oxygen; Temperature-programmed reduction; De–SO_2

1. Introduction

In the fluid catalytic cracking (FCC) process, SO_x (SO_2, SO_3) emissions are generated in the regenerator during the burning of the coke deposited on the surface of the FCC catalysts [1]. In order to reduce SO_x emissions from the regenerator of FCC unit, some of techniques can be used, for example, the flue gas treatment (FGT) and feedstock desulfurization technology (FDT) [2–5]. From an economical point of view, however, all of these are costly. Recently, it is believed that a better strategy for SO_x emission control is to add to the FCC catalyst a so-called sulfur-transfer catalyst that can adsorb SO_x to form sulfates under the oxidation atmosphere in the regenerator and then decomposes the formed sulfates into H_2S under the reduction atmosphere in the reactor and the stripper. Sulfide compounds are then treated in a modified Claus process to yield element sulfur [6–8]. The operation cost of using sulfur-transfer technique is only one-seventh and one-thirtieth of FDT and FGT, respectively [9].

Magnesium–alumina spinel materials are found to be the potential De–SO_x catalysts.

* Corresponding author. Tel. +52-5-6225129; Fax: +52-5-6161535; E-mail: wang_ja@fenix.ifisicacu.unam.mx

1381-1169/99/$ - see front matter
PII: S1381-1169(98)00205-2

Especially, when some transition metal ions such as Fe^{3+}, V^{5+} and Cu^{2+} ions, are introduced into the structures of magnesium–alumina spinel, the De–SO_x ability is obviously improved [10–12]. Since the high content of iron ion can promote the coke formation and vanadium ions can partially cause FCC catalysts deactivation during the catalytic cracking process if it is moved to the surface of the FCC catalysts, their contents, therefore, must be carefully controlled when they are used as promoters.

It is reported that rare earth metal oxides, such as CeO_2 and La_2O_3, can improve the De–SO_x activity of magnesium–alumina sulfur-transfer catalysts [13–15]. Rare earth metal oxides are widely applied in the catalysis field to improve the activity and selectivity or the thermal stability of the catalysts. A large number of papers are published on cerium oxide used in the area of environmental protection, for example, in automobile emission control [16–20]. However, the studies of rare metal oxides used as a promoter to enhance the De–SO_2 activity of sulfur-transfer catalysts are not sufficient yet.

Rare metal oxides supported on the surface of a sulfur-transfer catalyst may serve both to absorb the sulfur oxide and to assist in the transferring of sulfur oxides to the inorganic sulfates. In particular, the formation of the inorganic sulfates may result from an ability of the rare earth metal to catalyze the conversion of sulfur dioxide to sulfur trioxide [21]. Moreover, unlike the precious metals, such as Pt and Pd, rare earth metal oxides do not significantly enhance the formation of nitrogen oxides in the FCC process [21,22].

When CeO_2 is introduced onto the surface of magnesium–alumina spinel catalyst, the surface structure of the catalyst is strongly modified, which leads in an increment of the surface oxygen species adsorbed on the catalyst [23]. In the other hand, the De–SO_2 activity of catalyst was significantly affected by gaseous oxygen and surface adsorbed oxygen [24,25]. CeO_2 and surface oxygen species, therefore, take very important roles in the cycle of the oxidative adsorption of sulfur dioxide and the reductive desorption of adsorbed sulfur species in the FCC process using the sulfur-transfer technique for SO_x control. However, the effects of supported cerium oxide on surface oxygen property of the catalyst, in particular, the reducibility and recoverability of the surface oxygen species are not very clear.

In the present paper, we focus on the properties of the surface oxygen species and the roles of supported cerium oxide on both $MgAl_2O_4$ and $CeO_2/MgAl_2O_4$ catalysts during the De–SO_2 procedure. Temperature-programmed reduction (TPR) was used to determine the surface oxygen species and their adsorption ability, reducibility and recoverability. In order to compare the De–SO_2 abilities of the magnesium–alumina spinel and the cerium containing magnesium–alumina spinel catalysts, the tests for SO_2 adsorption or oxidative adsorption were carried out.

2. Experimental

2.1. Catalyst preparation

The magnesium–alumina spinel catalyst was prepared by the co-precipitation method (specific surface area $S_o = 110\ m^2/g$, pore volume $V_o = 0.2414\ cm^3/g$). The $CeO_2/MgAl_2O_4$ catalyst was prepared by impregnating the $MgAl_2O_4$ sample into the given concentration of the $(NH_4)_2Ce(NO_3)_6$ solution. The content of CeO_2 was ranged from 3 to 18 wt.%. The cerium supported magnesium–alumina catalyst was then dried at 120°C overnight and calcined at 700°C for 4 h.

2.2. Temperature-programmed reduction

The surface oxygen property was determined by means of TPR method in a quartz reactor coupled with a thermal conductivity detector.

The 0.1 mg sample was heated at a rate of 10°C/min under a stream of 50 ml/min of dry He from 20°C to 300°C. At 300°C, it was heated for 1 h. Then 10% H_2 in He was fed into the reactor at a rate of 50 ml/min. The TPD signal was recorded using a microcomputer lined with the measurement system. In the other cases, the samples were firstly pretreated at various conditions and then TPR analyses were carried out.

2.3. X-ray spectroscopy (XPS)

XPS measurement was performed on a PHI 550-ESCA/SEA spectrometer. Before the measurement, the sample was treated under a flow of He for 1 h at 300°C.

2.4. SO_2 adsorption or oxidative adsorption

A WRT-2 thermogravimetric analyzer, connected with a microcomputer, temperature-programmed controlling system and vacuum treatment system, was used to measure the weight change of the sample under the adsorption atmosphere. Typically a 10–20 mg sample was placed on the quartz sample pan. The standard experimental conditions for SO_2 adsorption or oxidative adsorption are as follows: adsorption temperature is 700°C; adsorption time is 30 min; in the case of SO_2 adsorption, 1.2 vol% SO_2 in N_2 was fed in a rate of 20 ml/min; in the case of SO_2 oxidative adsorption, a mixture of 5 vol% O_2 and 1.2 vol% SO_2 was fed in a rate of 20 ml/min.

3. Results and discussions

3.1. Surface oxygen species

The TPR spectra of different samples are shown in Fig. 1. On the $MgAl_2O_4$ sample, one peak centered at 400°C, and another peak located at 700°C, were observed (Fig. 1a). When 3 wt.% CeO_2 was supported on the $MgAl_2O_4$ sample, two peaks, α and β, were found (Fig. 1b). The area of peak α increased with the increasing of the CeO_2 content, remaining its position unchanged. When the CeO_2 content exceeded 8 wt.%, the peak α followed a decreasing trend. However, for the peak β, its area was almost unchanged. But its position, comparing to the position in the $MgAl_2O_4$ sample, shifted about 20, 50 and 60°C to the lower temperature when the ceria content reached 3, 5 and 8 wt.%. In addition, as the content of CeO_2 was more than 8 wt.%, a new peak γ at 760°C appeared, which gradually increased as the cerium content increased.

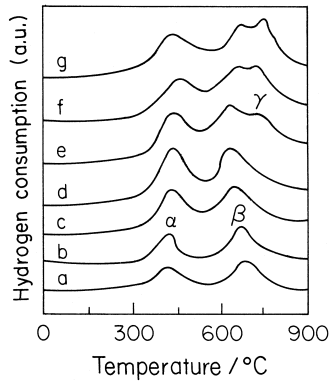

Fig. 1. TPR spectra of the different samples; (a) $MgAl_2O_4$; (b) 3 wt.% CeO_2 /$MgAl_2O_4$; (c) 5 wt.% CeO_2 /$MgAl_2O_4$; (d) 8 wt.% CeO_2 /$MgAl_2O_4$; (e) 12 wt.% CeO_2 /$MgAl_2O_4$; (f) 15 wt.% CeO_2 /$MgAl_2O_4$.

In general, the temperature corresponding to the central peak of consuming hydrogen (TPR peak) and the amount of consuming hydrogen are often used to characterize the different surface oxygen species and their reducibility. In our previous paper, the monolayer dispersion capacity of cerium oxide on the magnesium–alumina spinel catalyst was determined to be in the range of 7.5–8 wt.% CeO_2 by using both XRD and positron annihilation spectroscopy for chemical analysis (PASCA) techniques [23]. When CeO_2 content exceeded 8 wt.%, multilayer crystallite CeO_2 was formed on the surface of catalyst [23]. The peak γ was found on the samples containing more than 8 wt.% CeO_2, and its area increased with the increasing of the cerium oxide content; moreover, the centered

temperature of the peak γ was similar to that of the pure CeO_2 reduction [26]. Because the interaction between the supported multilayer CeO_2 and the support is very weak, which is supported by the measurements of the PASCA technique, its reduction property is hence similar to the one of the pure CeO_2. Therefore, it is deduced that the reduction of multilayers of CeO_2 crystals on the $CeO_2/MgAl_2O_4$ sample is responsible for the peak γ.

The position of the peak β observed in this work was similar to that reported by Lu and Wang [27], in their work, this peak was ascribed to the reduction of the surface lattice oxygen species in the sample containing ceria. The reduction of lattice oxygen on the pure CeO_2 crystal is often registered at higher temperature in TPR analysis [26]. When CeO_2 was loaded to the surface of the catalyst, if the cerium oxide content is less than the threshold value of monolayer dispersion, a strong interaction occurs between the CeO_2 and the support [23]. This strong interaction remarkably affects the surface structure of the catalysts, resulting in more oxygen vacancies being created. The properties of the surface oxygen, therefore, are significantly modified [23]. Probably the shift of the peak β to the low temperature was caused by this strong interaction. Hence, the peak β here was likely produced by the reduction of surface lattice oxygen species that were strongly affected by the interaction between the supported cerium oxide and the carrier.

In order to gain insight into the property of the α peak, the 8 wt.% $CeO_2/MgAl_2O_4$ sample was treated in a He stream of 50 ml/min at different temperatures for 30 min, and then the TPR measurements were carried out. The results are presented in Fig. 2. It was found that the pretreatment remarkably affected the peak α instead of the peak β. The higher the pretreatment temperature, the smaller the peak α is. Increasing the pretreatment temperature from 200, 300, 400 to 500°C resulted in the relative areas of the peak α being diminished from 9.5, 7.3, 3.6 to 1.0. All of those results reveal that

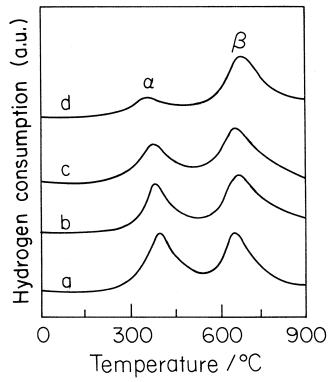

Fig. 2. TPR spectra of 8 wt.% $CeO_2/MgAl_2O_4$ sample; (a) 200°C; (b) 300 °C; (c) 400°C; (d) 500°C.

the α peak is caused by the reduction of the surface adsorbed oxygen species.

According to the results of XPS measurement, on the 8 wt.% $CeO_2/MgAl_2O_4$ sample, O_{1s} spectrum can be resolved into two different parts: 528.5–530.0 eV and 530.0–531.5 eV. The former was ascribed to the surface lattice oxygen and the latter was induced to the adsorbed oxygen species [28,29]. This result provides the further evidence for the above suggestion concerning the peak α.

3.2. Reducibility and recoverability of surface oxygen species

After the first TPR measurement, the $MgAl_2O_4$ and the 8 wt.% $CeO_2/MgAl_2O_4$ samples were cooled under a stream of He to the desirous temperatures and then 10% O_2 in N_2 was introduced for 30 minutes, following the second TPR measurements. For the $MgAl_2O_4$ sample (Fig. 3), the peak α and the peak β were observed at almost the same positions as showing in the fresh sample (Fig. 3a). When the sample was treated using oxygen at 50°C for 30 min, the area of the peak α, corresponding to the second TPR, is similar to that shown in the first TPR; the peak β, however, was smaller in comparison with the fresh sample. Although the peak β increased when the oxygen adsorption temperature increased, it did not reach the level shown on the fresh sample at the same tempera-

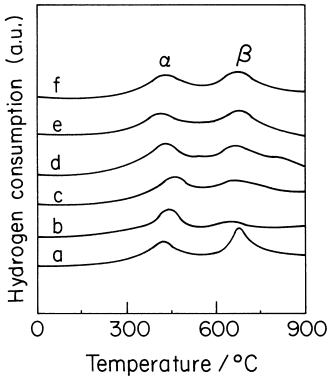

Fig. 3. TPR spectra of $MgAl_2O_4$ sample with different pretreatment; (a) fresh sample; (b–f) reduced samples were firstly treated by O_2 at 50, 200, 300, 500 and 700°C, respectively, then the second TPR measurements were operated.

ture. This result shows that on the $MgAl_2O_4$ sample, the recovery of surface lattice oxygen is more difficult at lower temperature and it is only partially recovered at temperature as high as 700°C.

Compared to the first TPR, the peak β appeared in the $CeO_2/MgAl_2O_4$ in the second TPR was larger, showing that the amount of adsorbed oxygen species increases (Fig. 4). This can be explained by the fact that more oxygen vacancies existed in the surface of the sample after it was reduced with hydrogen. These oxygen vacancies were filled with oxygen in the case of oxygen adsorption process, which leaded to more oxygen species being adsorbed on the surface of the sample. As shown in Fig. 4, although the peak β, corresponding to the $CeO_2/MgAl_2O_4$ sample, was still small when the sample was pretreated using oxygen at 50°C, it obviously increased at 200°C. At 500°C, the peak β reached the level of the first TPR on the fresh sample. These results suggest that the surface lattice oxygen is completely recovered.

The reduction of the surface lattice oxygen is shown in Eq. (1), where $O^{2-}(\text{latt})$ stands for oxygen lattice. Due to the electron neutrality, two electrons are suggested to be trapped in this vacancy. $V_o^{\cdot\cdot}$ stands for an oxygen vacancy with two free-like electrons.

$$O^{2-}(\text{latt}) + H_2(g) \rightleftharpoons H_2O + V_o^{\cdot\cdot} \quad (1)$$

When oxygen molecule adsorbed on the oxygen vacancy with two free-like electrons, the trapped electron can be captured to form adsorbed oxygen ion, which is illustrated as the Eq. (2):

$$1/2O_2(g) + V_o^{\cdot\cdot} \rightleftharpoons O^-(\text{ads}) + e^- \quad (2)$$

The adsorbed oxygen ion (O^-) captures another free-like electron and transfers to a lattice oxygen species. In such case, the reduced lattice oxygen is recovered (Eq. (3)):

$$O^-(\text{ads}) + e^- \rightleftharpoons O^{2-}(\text{latt}) \quad (3)$$

In the one hand, in comparison with the $CeO_2/MgAl_2O_4$ and $MgAl_2O_4$ samples, the peak α on the $CeO_2/MgAl_2O_4$ sample is larger. This suggests that the amount of adsorbed oxygen on the sample containing ceria is more. In the other hand, taking account of the facts that in the $CeO_2/MgAl_2O_4$ sample, the position of the peak β shifts to the lower temperature and this peak is recovered at 500°C, it is believed that the lattice oxygen on $CeO_2/MgAl_2O_4$ is very active with high recoverability. Therefore, cerium oxide loaded on the magnesium–alumina spinel catalyst enhances the ability of gaseous oxygen adsorption on the catalyst's surface and improves the recoverability of the surface lattice oxygen. Cerium oxide modifies the surface oxygen properties of the catalyst by improving the interaction between gaseous oxygen, adsorbed oxygen and lattice oxygen species.

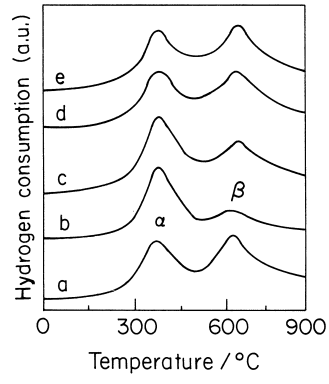

Fig. 4. TPR spectra of the 8 wt.% $CeO_2/MgAl_2O_4$ sample with different pretreatment; (a) fresh sample; (b–e) reduced samples were firstly treated by O_2 at 50, 200, 500 and 700°C, respectively; then the second TPR measurements were operated.

3.3. Effects of supported cerium and oxygen on the De–SO_2 activity

In the absence of oxygen, SO_2 adsorption on the $MgAl_2O_4$ and the 8 wt.% $CeO_2/MgAl_2O_4$ samples was carried out on a TGA experimental system. The results are shown in Figs. 5 and 6. At different adsorption temperatures, the initial rates of weight gain for SO_2 adsorption were similar for both the $MgAl_2O_4$ and the 8 wt.% $CeO_2/MgAl_2O_4$ samples. As the adsorption temperature increased, the rate of weight gain decreased in the $MgAl_2O_4$ sample. In such case, because no gas oxygen involved in the formation of the adsorbed sulfur species, the initial adsorption rate was mainly determined by the concentration of adsorbed sites existing on the surface of the catalyst. For the same catalyst, the number of the adsorbed sites is the same; therefore, the initial adsorption rates at different temperatures should be similar. However, because both weak and strong adsorbed SO_2 species coexisted on the surface of the catalyst, when the adsorption temperature increased, the weak adsorbed sulfur species would desorb from the surface of the catalyst, therefore, the total amount of the adsorbed SO_2 on the $MgAl_2O_4$ sample diminished at high adsorption temperature (Fig. 5) [30,31].

In the 8 wt.% $CeO_2/MgAl_2O_4$ sample, when SO_2 is adsorbed at the different temperatures, the order of weight gain is as follows:

$$W_{400^\circ C} > W_{600^\circ C} \approx W_{700^\circ C} > W_{500^\circ C} \quad (4)$$

At a high temperature, according to the results of TPR, the lattice oxygen in the sample is active due to the promoting action of cerium. This factor probably favors the strong chemisorption of SO_2 and hence partially offsets the effect of the desorption of weak adsorbed species at the higher adsorption temperature, consequently, making the sequence of weight gain very change.

At the same adsorption time and temperature, when oxygen is present in the fed stream, the rate of the weight gain of SO_2 adsorption is about 3–4 times than that in the absence of oxygen (Figs. 7 and 8). Unlike the results obtained in the case of oxygen absence, for both the $MgAl_2O_4$ and the $CeO_2/MgAl_2O_4$ sam-

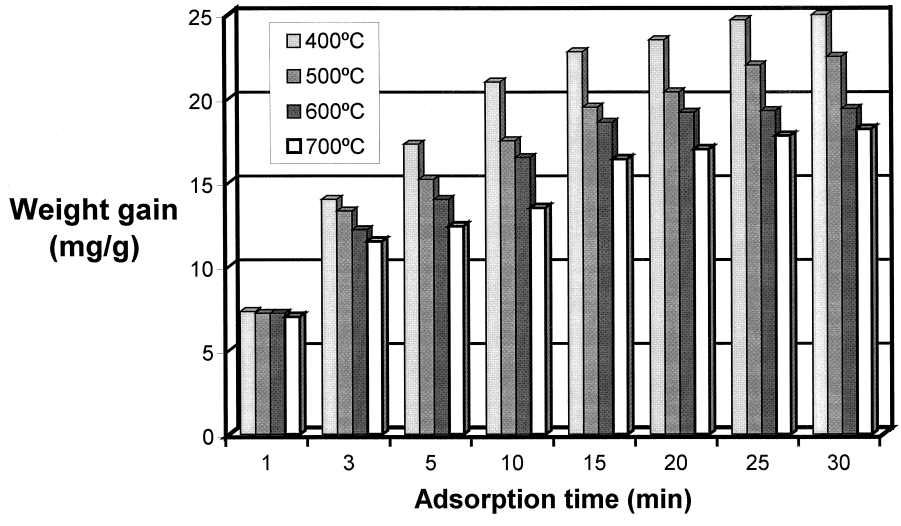

Fig. 5. Weight gain as a function of SO_2 adsorption time. The SO_2 is adsorbed on the $MgAl_2O_4$ sample at 400, 500, 600 and 700°C for 30 min. Oxygen is absent in the fed gases.

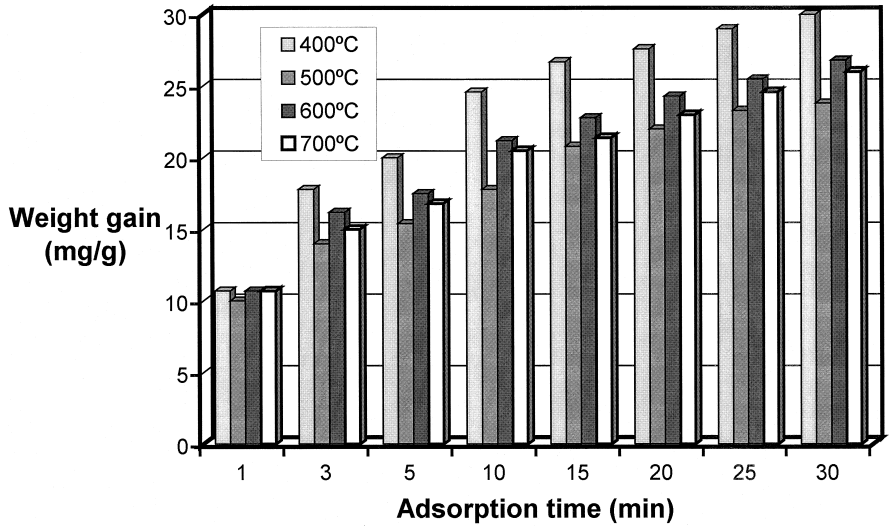

Fig. 6. Weight gain as a function of SO_2 adsorption time. The SO_2 is adsorbed on the 8 wt.% $CeO_2/MgAl_2O_4$ sample at 400, 500, 600 and 700°C for 30 min. Oxygen is absent in the fed gases.

ples, when oxygen contains in the fed stream, the weight gain shows the following order (Eq. (5)):

$$W_{700°C} > W_{600°C} > W_{500°C} > W_{400°C} \quad (5)$$

It is noteworthy that a significant difference between the presence and absence of oxygen in the fed stream is that during the adsorption procedure, molecular oxygen and sulfur dioxide are simultaneously adsorbed on the surface of the catalyst when oxygen is added. This means that the adsorption of both molecular oxygen and SO_2 is responsible for the observed weight gain in the case of oxygen containing in the

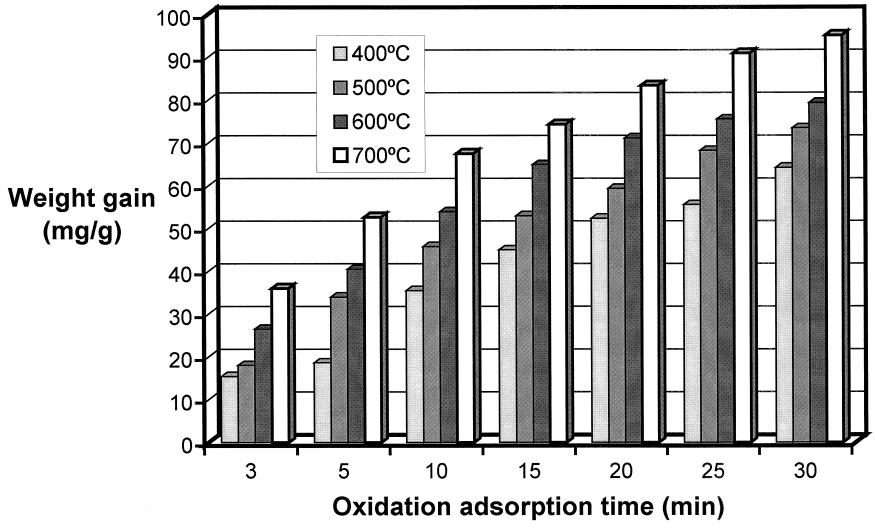

Fig. 7. Weight gain as a function of SO_2 oxidative adsorption time. The SO_2 is adsorbed on the $MgAl_2O_4$ sample at 400, 500, 600 and 700°C for 30 min. The fed gases contain oxygen.

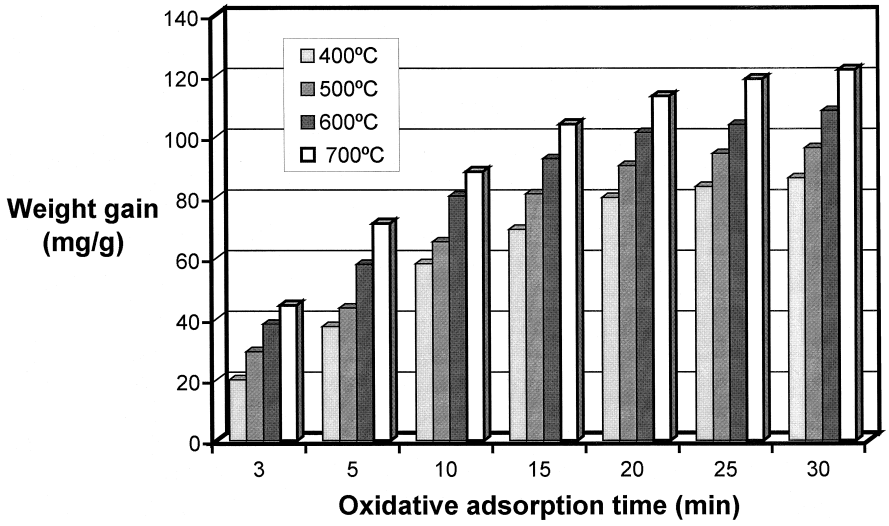

Fig. 8. Weight gain as a function of SO_2 oxidative adsorption time. The SO_2 is adsorbed on the 8 wt.% $CeO_2/MgAl_2O_4$ sample at 400, 500, 600 and 700°C for 30 min. The fed gases contain oxygen.

inlet gases. However, the adsorption of oxygen and sulfur dioxide on the surface is rapid and therefore it is difficult to determine their individual contribution to the weight gain. Since the number of the sites for oxygen adsorption (oxygen vacancies) is less than the sites for SO_2 adsorption (oxygen lattices) and the molecular weight of SO_2 is two times than that of oxygen molecule, the contribution of oxygen adsorption to the weight gain is relatively smaller compared to the SO_2 adsorption. This is supported by the experimental results that the weight gain is no more than 17 mg/g during the 30 min of oxygen adsorption on the catalysts [32]. In fact, the SO_2 oxidative adsorption is a process accompanying the reaction between the adsorbed oxygen ion and the adsorbed sulfur species for forming sulfate. Therefore, the weight gain mainly reflects the abilities of sulfur dioxide adsorption or oxidative adsorption on the catalysts.

It is found that the weight gain of the sulfur dioxide adsorption on the 8 wt.% $CeO_2/MgAl_2O_4$ sample is significantly more than that on $MgAl_2O_4$ sample. The mean rate of weight gain as a function of the adsorption temperature for these two samples were plotted in Fig. 9. Two lines with different liners were acquired. According to Arrhenius equation, the activation energies of sulfur dioxide oxidative adsorption on both $MgAl_2O_4$ and 8 wt.% $CeO_2/MgAl_2O_4$ samples are 20 kJ/mol and 11 kJ/mol, respectively. This result clearly shows that the activation energy of sulfur dioxide oxidative adsorption is reduced about 0.8 times when cerium

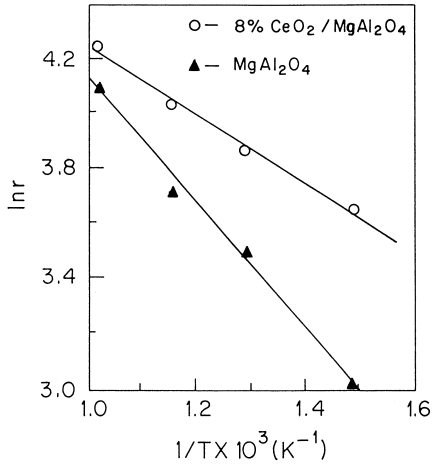

Fig. 9. lnr as a function of $1/T$; (a) 8 wt.% $CeO_2/MgAl_2O_4$ sample; (b) $MgAl_2O_4$ sample.

oxide is loaded on the magnesium–alumina spinel catalyst. The activity of SO_2 oxidative adsorption on the sample containing cerium is hence improved.

4. Conclusions

Three different peaks of consuming hydrogen in the $CeO_2/MgAl_2O_4$ catalysts were determined, which were respectively responsible for the reduction of the three different oxygen species—surface adsorbed oxygen, surface lattice oxygen and the oxygen species corresponding to the multilayer CeO_2 crystalline on the surface of catalysts.

The properties of the surface oxygen species were remarkably modified when rare oxide CeO_2 was supported on magnesium–alumina spinel catalyst. Three different roles of cerium oxide were found: first, it increased the amount of surface adsorbed oxygen; second, it reduced the reduction temperature of surface lattice oxygen and the third is that it promoted the recoverability of the surface adsorbed oxygen and lattice oxygen species.

By means of the interaction and transformation between the gaseous oxygen, surface adsorbed oxygen and surface lattice oxygen, supported cerium oxide can cause a reduction of the activation energy of sulfur dioxide oxidative adsorption on the catalyst and hence improved the De–SO_2 activity of magnesium–alumina spinel catalyst.

Acknowledgements

The authors are grateful to the National Nature Science Foundation of China and China Jinling Petrochemical Cooperation for their financial support.

References

[1] A. Corma, E.L. Kugler, Progress in FCC Catalysts, Catalytica Studies Division, 1992.
[2] P.S. Lowell, K. Schwitzgebel, T.B. Parsons, K.J. Sladek, Ind. Eng. Chem. Proc. Des. Dev. 10 (1971) 384.
[3] R.J. Best, J.G. Yates, Ind. Eng. Chem. Proc. Des. Dev. 16 (1977) 347.
[4] F.M. Dautzenberg, J.E. Naber, A.J. Ginneken, Chem. Eng. Prog. 67 (1971) 86.
[5] N.W. Frank, G.A. Miller, D.A. Reed, Environ. Prog. 6 (1987) 17.
[6] J.W. Byrne, B.K. Spernello, Oil Gas J. 15 (1984) 101.
[7] J.S. Yoo, A.A. Bhaffracharga, C.A. Radlowasi, Ind. Eng. Chem. Res. 30 (1991) 1444.
[8] A.A. Bhattachryya, G.M. Woltermann, J.S. Yoo, J.A. Karch, W.E. Cormier, Ind. Eng. Chem. Res. 27 (1988) 384.
[9] D.P. MxArthur, H.D. Simpson, K. Baron, Oil Gas J. (1983) 70.
[10] A. Corma, A.E. Palomares, F. Rey, Appl. Catal. B 4 (1994) 29.
[11] J.S. Yoo, A.A. Bhaffracharga, C.A. Radlowski, Appl. Catal. B 1 (1992) 169.
[12] F.T. Clark, M.C. Springman, D. Winncox, E. Wachs, J. Catal. 139 (1993) 1.
[13] R.J. Bertolacini, U.S. Patent, 4 381 991 (1986).
[14] A. Bhaffracharga, G.M. Woltermann, J.A. Yoo, W.F. Cornier, ACS Meeting, 30 Aug.–4 Sept., 1987.
[15] J.A. Wang, C.L. Li, Y.Y. Dai, X.P. Gao, Acta Physico–Chemica Sinica 7 (1994) 581.
[16] Y.F.Y. Yao, J. Catal. 87 (1984) 154.
[17] H.C. Yao, Y.F.Y. Yao, J. Catal. 86 (1986) 125.
[18] Laachir, V. Perrichon, J. Chem. Soc., Faraday Trans. 87 (1991) 1601.
[19] J.M. Herrmann, C. Hoang-Van, L. Dibansa, R. Harivololona, J. Catal. 159 (1996) 361.
[20] J.M. Herrmann, E. Romaroson, J.F. Tempereand, M.F. Guilleux, Appl. Catal. 53 (1989) 117.
[21] E.J. Demmel, 1993 NPPA Annual Meeting, San Antonio, TX, March 21–23, 1993.
[22] J.C. Summers, Environ. Sci. Technol. 13 (1979) 321.
[23] J.A. Wang, L.F. Chen, C.L. Li, J. Mater. Sci. Lett. 17 (1998) 533.
[24] M. Waqif, O. Saur, J.C. Lavalley, Appl. Catal. 71 (1991) 319.
[25] A. Morrow, Mater. Chem. Phys. 19 (1988) 147.
[26] G. Balducci, P. Fornasiero, Catal. Lett. 33 (1995) 193.
[27] G.Z. Lu, R. Wang, J. Catal. 12 (1991) 261, (China).
[28] J.A. Wang, PhD Thesis, East China University of Science and Technology, Shanghai, China, (1995) 106.
[29] A. Davydov, Kinet. Katal. 20 (1979) 1506.
[30] J.A. Wang, Z.L. Zhu, C.L. Li, J. Mol. Catal. (in press).
[31] S.W. Nam, G.R. Gavalas, Appl. Catal. 55 (1989) 193.
[32] J.A. Wang, C.L. Li, in preparation.